Accepted Article

Title: Coordination of Actinide Single Ions with Deformed Graphdiyne: Strategy on Essential Separation Processes in Nuclear Fuel Cycle

Authors: Tianyu Yuan, Shijie Xiong, and Xinghai Shen

This manuscript has been accepted after peer review and appears as an Accepted Article online prior to editing, proofing, and formal publication of the final Version of Record (VoR). This work is currently citable by using the Digital Object Identifier (DOI) given below. The VoR will be published online in Early View as soon as possible and may be different to this Accepted Article as a result of editing. Readers should obtain the VoR from the journal website shown below when it is published to ensure accuracy of information. The authors are responsible for the content of this Accepted Article.

WILEY-VCH

RESEARCH ARTICLE

Coordination of Actinide Single Ions with Deformed Graphdiyne: Strategy on Essential Separation Processes in Nuclear Fuel Cycle

Tianyu Yuan, Shijie Xiong and Xinghai Shen*

Beijing National Laboratory for Molecular Sciences, Fundamental Science on Radiochemistry and Radiation Chemistry Laboratory, Center for Applied Physics and Technology, College of Chemistry and Molecular Engineering, Peking University, Beijing 100871, P. R. China.
* Corresponding Author: Prof. Xinghai Shen, xshen@pku.edu.cn
Supporting information for this article is given via a link at the end of the document.

Abstract: The coordination of actinides, lanthanides, as well as strontium and cesium with graphdiyne (GDY) was studied by experiments and theoretical calculations. On the basis of experimental results and/or theoretical calculations, it was suggested that Th^{4+}, Pu^{4+}, Am^{3+}, Cm^{3+} and Cs^+ exist in single ion states on the special triangle structure of GDY with various coordination patterns, in which GDY itself is deformed in different manners. Both experiments and theoretical calculations strongly support that UO_2^{2+}, La^{3+}, Eu^{3+}, Tm^{3+} and Sr^{2+} are not adsorbed by GDY at all. The distinguished adsorption behaviors of GDY afford an important strategy for highly selective separation between actinides and lanthanides, Th^{4+} and UO_2^{2+}, Cs^+ and Sr^{2+} in nuclear fuel cycle. Also, the present work sheds light on an approach to explore the unique functions and physicochemical properties of actinides in single ion states.

Introduction

Two-dimensional polymer carbon materials are currently one of the most active research fields in materials science. The synthesis and separation of new carbon isotopes of different dimensions have become the focus of research in the past two or three decades. Because the carbon-carbon triple bond formed in the *sp* hybrid has the advantages of linear structure, no *cis-trans* isomers, and high conjugation, it is of great importance to obtain a new allotrope of carbon with *sp* hybrid[1]. In 2009, Li's group[2] successfully synthesized GDY on the surface of copper foil. Due to the *sp* and *sp²* hybrid electronic and layered two-dimensional planar structure, it has rich carbon chemical bonds and large conjugates. The system, as well as the large triangular gaps, have drawn great attention and interest from research groups in different fields around the world. After this, in 2015, Zhou *et al.*[3] changed the catalytic site through an improved Glaser-Hay coupling reaction, to synthesize a new structure of GDY nano-wall. In 2017, Matsuoka and collaborators[4] prepared extremely thin graphitic nanosheets through gas-liquid two-phase reaction and immiscible liquid-liquid two-phase reaction. So far, GDY has witnessed its applications in various fields[5] such as energy storage[6], catalysis[7], solar energy[8], biological sensing or detection[9], and environment[10].

Although the high complexation activity of GDY has been extensively investigated at this stage[1], there are few studies on its structural deformation when coordinating with ions. Lu and co-workers[11] verified the alkene-alkyne complex transition in GDY responsible for the high-performance of electrochemical actuators. Li *et al.*[12] investigated the electronic structure and stability of the transition-metal-adsorbed GDY clusters by means of density

functional theory calculations, which revealed that the GDY clusters with partially filled 3*d* orbitals have a distorted in-plane conjugated framework. It seems that the investigation on the deformation in the structure of GDY is essential for deep understanding its physicochemical properties. Theoretical calculations on the natural periodic structure of GDY showed that the distance between the centres of adjacent triangle structure is far longer than that required for chemical bonding[13]. Therefore, due to the special nanopores and large π bond properties of GDY, the combined single-ion or single-atom states occur, which is favourable to various applications[14].

The applications of single ions in energy storage materials, single ion magnets and catalyses are the focus of research in recent years[15]. Simon *et al.*[16] reviewed the current states of lanthanides, uranium and neptunium single ion magnets. The research concerning actinides commented in this review was mainly on U(III), U(V) and Np(V). The ligands for actinide single ion magnets mainly include borate esters and other highly anisotropic, strongly axially coordinated ones. To the best of our knowledge, there have been no reports on the interaction between GDY and actinides in the literature yet. Thus, we suppose that insight into the actinides single ion state in GDY is theoretically and practically important.

Separation between actinides and lanthanides is one of the hottest topics in the spent nuclear fuel cycle. In particular, because the similar chemical behaviours between actinides and lanthanides, and the concentrations of lanthanides are 20 to 50 times higher than that of minor actinides, the separation between trivalent actinides and lanthanides ions is very difficult[17]. So far, researchers have made great effects on the separation by liquid-liquid extraction and solid-phase extraction. In liquid-liquid extraction, a significant amount of research is being carried out worldwide to develop suitable ligands, like mixed 'N, O' donor ligands[18], 'N' donor ligands[19] and 'S' donor ligands[20]. However, in the specific application process, it was found that some ligands with good separation effect have insufficient solubility in commonly used organic solvents, and some other ligands may be emulsified during the extraction process. These all lead to a decrease in the efficiency of liquid-liquid extraction. The application of solid phase extraction has also received widespread attentions. By this method, the separation was mainly achieved by grafting selective ligands to different substrates including polymer resin[21], silica gel[22], diatomite[23], etc. However, limited by the mechanical strength of graft material or undifferentiated adsorption of some substrates, it is difficult to completely separate actinides from lanthanides, especially for trivalent actinides. Moreover, as a fertile material, thorium

RESEARCH ARTICLE

has important application value in the field of nuclear energy. However, whether in ore or thorium-base spent fuel, it often coexists with uranium. The separation between thorium and uranium is conducive to the efficient use of resources[24]. [137]Cs and ^{90}Sr are the main radioactive and heat release nuclides in spent fuel, so the extraction of ^{137}Cs and ^{90}Sr in high-level waste liquid can effectively reduce the radiation and thermal effects of spent fuel[25]. However, ^{137}Cs and ^{90}Sr are both raw materials of radiation sources. Thus, the further separation between Cs^+ and Sr^{2+} is of great significance[26]. Although there have been some researches on extraction of Cs^+ or Sr^{2+} by using crown ethers[27] or calixarene-crown ethers[28], it is still difficult to realize a complete separation between Cs^+ and Sr^{2+} during these extraction processes. Therefore, it is demanding to explore a material with highly selective adsorption capability and excellent mechanical properties. Hopefully, the GDY is a good candidate for such purpose.

Results and Discussion

Adsorption experiments of GDY

The synthesis of GDY and its characterization using Raman spectroscopy and SEM are described in the supporting information. Figure 1(A) shows that GDY coated on copper has obvious adsorption effect on Th^{4+} and Cs^+ but not on Sr^{2+}, UO_2^{2+}, La^{3+}, Eu^{3+} and Tm^{3+} at all. For comparison, copper foil itself was also added to the solution to determine the adsorption capacity. It is clear that in Figure 1(B,C) copper foil itself has adsorption capacity for both Th^{4+} and UO_2^{2+} as well as Cs^+ and Sr^{2+} in the mixed solutions, which is due to the oxidation groups existing on the surface of the copper foil. However, when the copper foil is coated with GDY, it exhibits an adsorption effect only on Th^{4+} or Cs^+. This indicates that the copper foil is completely covered with GDY and the adsorption results from GDY only. In order to examine the effect of the initial concentrations of Th^{4+} or Cs^+, the isothermal adsorption curve is shown in Figure 2(A,B). It can be seen that the adsorption of Th^{4+} or Cs^+ increases with the concentration of initial solution. The isothermal adsorption data were analyzed with the Langmuir and Freundlich models. The corresponding fitting results, presented in Table S1 (Supporting information), suggest that the Langmuir model is more suitable than Freundlich model. The q_m values of GDY coated on copper to Th^{4+} and Cs^+, calculated by Langmuir model, were 33.5 ± 4.2 and 12.7 ± 1.1 mg/g, respectively.

Spectral characterization of the interaction between GDY and ions

In the study of the mechanism of the interaction between Th^{4+} and GDY, XPS spectroscopy was used. Figure 3(A) shows the XPS spectra obtained from GDY before and after Th^{4+} adsorption, respectively. After adsorption, a new pair of peaks attributed to Th $4f_{7/2}$ and $4f_{5/2}$ appear, which confirms the successful adsorption of Th^{4+} on GDY. Comparing the XPS spectrum of $Th(NO_3)_4$ with that of Th^{4+} adsorbed on GDY, the obvious shift of the peaks of Th^{4+} can be found

(Figure 3(B)). The $4f_{7/2}$ and $4f_{5/2}$ binding energies of $Th(NO_3)_4$ are 336.0, 345.2 eV, respectively, and that of Th^{4+} adsorbed on GDY are clearly down-shifted by 0.8 eV (from 336.0 to 335.2 eV) and 1.1 eV (from 345.2 to 344.1 eV) compared with those of $Th(NO_3)_4$. The decrease in binding energies provides a direct evidence that Th^{4+} can receive electrons from GDY and indicates the strong binding of Th^{4+} to the sp-hybridized carbon atoms in GDY. The new peaks of Th^{4+} in XPS spectrum (Figure 3(B) inset, 343.4 and 334.4 eV) may be due to the difference of the single ion state of Th^{4+} adsorbed directly on the triangle structure of GDY from its aggregation state surrounding GDY.
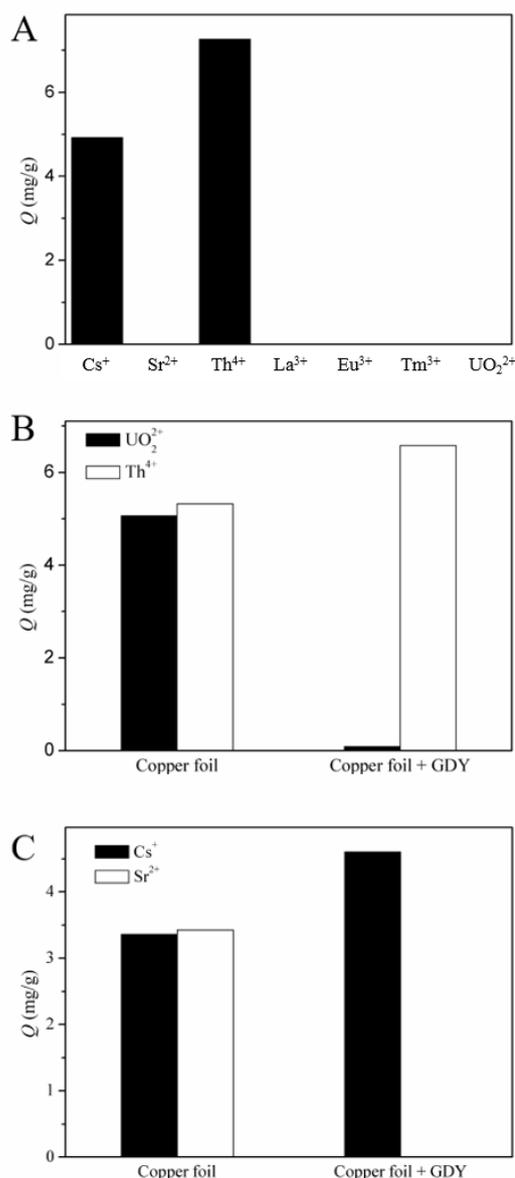
Figure 1 (A) The adsorption capacity of GDY coating copper foil towards Cs^+, Sr^{2+}, Th^{4+}, UO_2^{2+}, La^{3+}, Eu^{3+} and Tm^{3+}, respectively (100 mg/L). (B) The adsorption selectivity of copper foil itself and GDY coating copper foil in the mixed solution of Th^{4+} and UO_2^{2+}. The concentrations of Th^{4+} and UO_2^{2+} are 100 mg/L, respectively. (C) The adsorption selectivity of copper foil itself and GDY coating copper foil in the mixed solution of Cs^+ and Sr^{2+}. The concentrations of Cs^+ and Sr^{2+} are 100 mg/L, respectively.

2
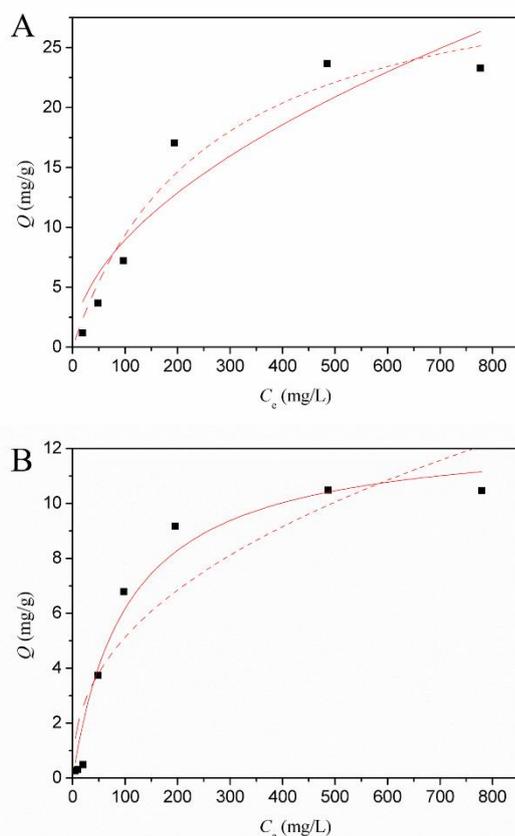
Figure 2 (A) The adsorption isotherm of GDY to Th^{4+} (Langmuir model: red dotted line, Freundlich model: red solid line). (B) The adsorption isotherm of GDY to Cs$^+$ (Langmuir model: red dotted line, Freundlich model: red solid line).

Figure 3(C) shows the XPS spectra obtained from GDY before and after Cs$^+$ adsorption, respectively. After adsorption, a peak attributed to Cs 3d appears, which confirms the successful adsorption of Cs$^+$ on GDY. Comparing the XPS spectrum of CsCl with that of Cs$^+$ adsorbed on GDY, the obvious shift of the peaks of Cs can be found (Figure 3(D)). The 3d binding energies of CsCl are 725.0, 723.7 eV, respectively, and that of Cs$^+$ adsorbed on GDY are clearly down-shifted by 0.5 eV (from 725.0 to 724.5 eV) and 2.5 eV (from 723.7 to 721.2 eV) compared with that of CsCl. The decrease in binding energies provides a direct evidence that Cs$^+$ can receive electrons from GDY and indicates the strong binding of Cs$^+$ to the *sp*-hybridized carbon atoms in GDY.

The Raman spectra of the conjugated diyne links obtained from GDY before and after adsorption of Th^{4+} were measured, which are illustrated in Figure 4. It can be clearly seen that the peak at 2170 cm^{-1} is broadened after adsorption, which could be decomposed into three subpeaks: 2145.0, 2170.0 and 2198.9 cm^{-1}. It was reported that when metal ions coordinate with the C≡C bond, the frequency of the C≡C stretching vibration decreases[29]. The peak of 2198.9 cm^{-1} will be analysed later in the article. Therefore, combining the results of XPS and Raman spectroscopy, it can be concluded that Th^{4+} was adsorbed on the triangle structure of GDY by interaction with C≡C.
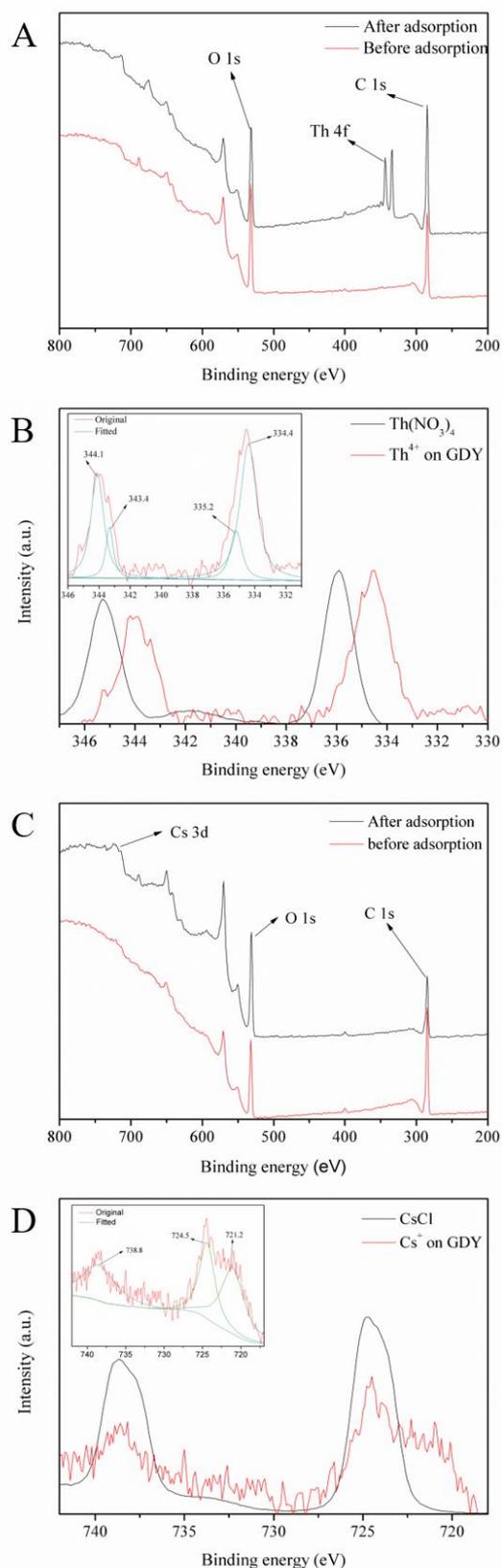
Figure 3. (A) The XPS spectra of GDY after and before adsorption of Th^{4+}. (B) The XPS spectrum of Th(NO$_3$)$_4$ and that of Th^{4+} adsorbed on GDY (Inset: the XPS spectrum and curve fitting of Th^{4+} adsorbed on GDY). (C) The XPS spectra of GDY after and before adsorption of Cs$^+$. (D) The XPS spectrum of CsCl and that of Cs$^+$ adsorbed on GDY (Inset: the XPS spectrum and curve fitting of Th^{4+} adsorbed on GDY).

3

RESEARCH ARTICLE
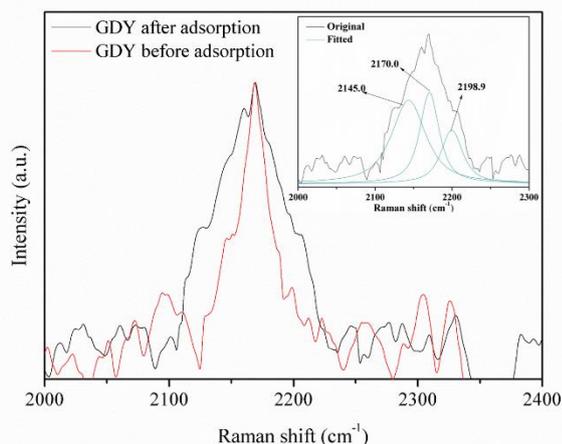
Figure 4. The Raman spectra of the conjugated diyne links after and before adsorption of Th^{4+} (Inset: curve fitting of the Raman spectrum after Th^{4+} adsorption).

Theoretical calculation of the interaction between GDY and ions

To further study the interaction between GDY and different ions, we choose Th^{4+}, UO$_2^{2+}$ Pu^{4+}, Am^{3+}, Cm^{3+}, La^{3+}, Eu^{3+}, Tm^{3+}, Cs$^+$ and Sr^{2+} as the target metal ions. It would be hard to get a stable structure if UO$_2^{2+}$ were adsorbed by GDY. The nitrate is the commonly used ligand in the extraction processes in nuclear fuel cycle. From several calculations about different numbers of nitrates, we found that the tetravalent and trivalent actinides adsorbed on GDY with two, one coordinated nitrates, respectively, are the stable structures. The selected actinides adsorbed by GDY are displayed in Figure 5. For Am^{3+}, Cm^{3+} and Pu^{4+}, it is obvious that the triangle structures of GDY get depressed, which are in contrast to the protruded local structure in the presence of Th^{4+}. The bond lengths and distortion degree of these structures are listed in Table 1. From Table 1, one can find that all of three sides in the triangle structure of GDY are significantly deformed by the coordination of Am^{3+}, Cm^{3+} and Pu^{4+}, while only two sides are curved to some extent in the presence of Th^{4+}. The covalent bonds have saturability and directivity, while electrostatic interactions do not have. For actinides adsorption, it is clear that only specific C atoms are much closer to actinides than other C atoms. These specific closer C atoms are in special directions in the space. These properties show obviously the saturability and directivity of covalent bonds. For Cs$^+$ adsorption, the GDY is deformed slightly and the deformation degree of three sides of GDY is similar. These features could not reflect the saturability and directivity of covalent bonds. Therefore, in Cs$^+$ adsorption, the electrostatic interaction is predominated, while this is not the case for the adsorption of other ions in this work. It is electrostatic interaction that leads to the attraction between Cs$^+$ and GDY. There is no covalent bond between Cs$^+$ and GDY. The adsorption energy in vacuum, hydration energy and adsorption energy in solution for actinides (Th^{4+}, Pu^{4+}, Am^{3+}, Cm^{3+}), lanthanides (La^{3+}, Eu^{3+}, Tm^{3+}) Cs$^+$ and Sr^{2+} are present in Table 2. The calculation results reveal that all the Cs$^+$, Sr^{2+}, selected actinides and lanthanides could be adsorbed by GDY in vacuum state. Taking the hydration

energy into account, the positive adsorption energy in solution suggests that Sr^{2+} and trivalent lanthanides could not be adsorbed by GDY in water. Meanwhile, the structural optimization of UO$_2^{2+}$ could not converge indicating no adsorption of UO$_2^{2+}$ on GDY. On the contrary, the actinides could be attracted with negative adsorption energies in solution, *i.e.* −361, −651, −688 and −634 kJ/mol for Th^{4+}, Pu^{4+}, Am^{3+} and Cm^{3+}, respectively. Same is Cs$^+$ with negative adsorption energy of −111 kJ/mol in solution. The disattraction of Sr^{2+} and lanthanides are compatible with experimental results. For actinides and lanthanides, it is the 5*f* electrons feeding back that makes trivalent actinides different from trivalent lanthanides. For lanthanides, the 4*f* electrons are too local to feed back to GDY.
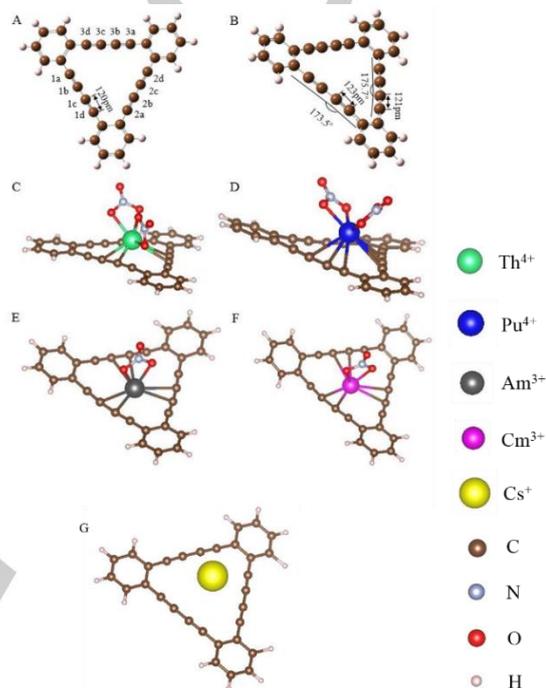
Figure 5 (A) Triangle structure of a GDY unit; (B) The changes of bond length and sides bending for the GDY triangle structure coordinating with Th^{4+} (Th^{4+} and nitrates omitted). Sides 1 and 2 are bended at the 1c and 2c carbon atoms, respectively; C, D, E, F, G illustrate local structures of GDY coordinating Th^{4+}, Pu^{4+}, Am^{3+}, Cm^{3+}, Cs$^+$ respectively. There is no covalent bonds between Cs$^+$ and GDY, because the Cs+ is adsorbed through electrostatic interaction.

Deformation of GDY combining different actinide ions

Some previous research[32] investigated single atom (V, Cr, Mn, Fe, Co, Mo) adsorbed on GDY. In these works, the single d-block metal atom is bonded with two sides of triangle structure of GDY and resides in an angle of the triangle structure. In this work, the tetravalent actinide single ion is also bonded with two sides of the triangle structure of GDY. However, due to the large volume of the actinides and the coordinated nitrates, the positions of actinides ions are much closer to the center of the triangle structure of GDY, which is different from the situation in the previous works. As shown in Figure 5, Th^{4+} is adsorbed on the triangle structure of GDY with two sides deformed. The bended degrees of two sides are 6.5° and 4.3°, respectively. The bending phenomenon and the blue shift of the peaks in the Raman

4

RESEARCH ARTICLE

spectrum both show that the GDY has been deformed. In Yang's research, the deformation of carbon conjugated system can blue shift of the peaks in the Raman spectrum[33]. However, GDY shows different deformation modes when combining other actinides (Figure 5). The distinction of the deformation of GDY might result from the difference in the electronic structure of actinides. The Pu^{4+}, Am^{3+}, Cm^{3+} ions are with $5f^4$, $5f^6$, $5f^7$ open-shell electronic structures, respectively, while Th^{4+} is a closed shell ion without $5f$ electrons. The actinides with $5f$ open shell may feed their open-shelled $5f$ electrons back to the conjugated system of the GDY. Both Pu^{4+} and Th^{4+} are bonding with two sides of the triangle structure. Compared with the structure of GDY in the presence of Th^{4+}, the side 3 in Pu^{4+} adsorbed GDY deforms evidently. It is the open-shelled $5f$ electrons that make the difference. The open-shelled $5f$ electrons of Pu^{4+} are fed back to GDY and destroy the conjugation of GDY, which influences the third side indirectly. Compared with local structures of Am^{3+} adsorbed GDY and Cm^{3+} adsorbed GDY, the local structure of Pu^{4+} adsorbed GDY is less deformed. The reason is that Am^{3+} and Cm^{3+} have more $5f$ electrons and two nitrates coordinating with Pu^{4+} impose more steric hindrance. The calculations show that the trivalent actinides bond with all three sides of the triangle structure of GDY, while the tetravalent actinides only bond with two sides. This can be understood in terms of the fact that the tetravalent actinides are smaller than the trivalent actinides and two nitrates get much steric hindrance. Compared with Ref. 12, it can be found that the deformation tendency of GDY after combining the f-layer electrons is obviously different from that of the d-layer electrons.

Actinide single ion states on GDY

In order to explain the split of XPS peaks of Th^{4+} adsorbed on GDY, we implemented a calculation on a $Th(NO_3)_4 \cdot 3H_2O$ and a cluster of 4 $Th(NO_3)_4 \cdot 3H_2O$. The calculated $4f$ energy of $Th(NO_3)_4 \cdot 3H_2O$ is 333.4 eV and that of 4 $Th(NO_3)_4 \cdot 3H_2O$ cluster is 333.7 eV. The remarkable difference can be ascribed to the fact that the $4f$ orbitals in the cluster or crystal are overlapped leading to a small effect of the energy. The above analyses support the phenomenon that the XPS peak of Th^{4+} in single ion state shifts towards the low field. Combining the results of experiments and calculation, we believe that GDY is an effective substrate for the presence of single ions of the selected actinides in this work. To the best of our knowledge, this is the first study on the coordination between actinide ions and GDY, and also the first observation and confirmation of single ion state of Th^{4+}, Pu^{4+}, Am^{3+} and Cm^{3+} on GDY through both experiments and theoretical calculations. Moreover, although there have been some studies on actinides catalysing terminal alkyne bond[34], the coordination of actinides ions with alkyne bond is reported for the first time in this work. Similar to the function of single-ion or single-atom catalysts as mentioned above, actinide single ions adsorbed on GDY can also be used as catalysts in further researches, which may pave the way of the utility of the special catalyses of actinides. In addition, GDY can be modified by oxidation or substitution of different atoms[1]. These modifications may enhance the magnetic anisotropy of GDY adsorbed actinide single ions, thus enabling the syntheses of single ion magnets[35]. It is speculated that GDY can become an ideal substrate for some actinide single ion magnets.

Table 1. The bond length (pm) and bended degree of side when GDY combining tetravalent or trivalent actinides M^{n+} (Th^{4+}, Pu^{4+}, Am^{3+}, Cm^{3+}, Cs^+). The sequence numbers of carbon atoms are the same as in Figure 3A. The O1, O2, O3 and O4 are four atoms from two nitrates.

M^{n+}	Th^{4+}	Pu^{4+}	Am^{3+}	Cm^{3+}	Cs^+
M^{n+}-1b	269	302	299	295	--
M^{n+}-1c	246	289	291	294	--
M^{n+}-1d	--	321	--	--	--
M^{n+}-2a	--	306	--	--	--
M^{n+}-2b	307	284	286	294	--
M^{n+}-2c	324	316	290	294	--
M^{n+}-3b	--	--	289	283	--
M^{n+}-3c	--	--	291	285	--
M^{n+}-O1	249	235	242	240	--
M^{n+}-O2	247	239	241	240	--
M^{n+}-O3	250	236	--	--	--
M^{n+}-O4	254	237	--	--	--
Bended degree of Side 1	6.5°	6.2°	8.9°	11.2°	2.6°
Bended degree of Side 2	4.3°	6.9°	11.4°	11.9°	1.6°
Bended degree of Side 3	--	8.4°	7.4°	6.2°	2.7°

Table 2. The adsorption energy in vacuum, hydration energy and adsorption energy in solution for M^{n+} (Th^{4+}, Pu^{4+}, Am^{3+}, Cm^{3+}, La^{3+}, Gd^{3+}, Tm^{3+}, Cs^+, Sr^{2+}). All energy values are in kJ/mol.

M^{n+}	$E_{adsorb, vac}$	E_{hyd}	$E_{adsorb, sol}$
Th^{4+}	− 6828	− 5815[a]	− 361
Pu^{4+}	− 7863	− 6560[a]	− 651
Am^{3+}	− 4328	− 3288[b]	− 688
Cm^{3+}	− 4303	− 3317[b]	− 634
La^{3+}	− 2974	− 3145[a]	523
Eu^{3+}	− 3295	− 3375[a]	432
Tm^{3+}	− 3341	− 3515[a]	526
Cs^+	− 413	− 250[a]	− 111
Sr^{2+}	− 1683	− 1380[a]	49

[a] Taken from Ref. 30. [b] Taken from Ref. 31.

Separation between actinides and lanthanides, Th^{4+} and UO_2^{2+}, Cs^+ and Sr^{2+} by GDY

Separation between actinides and lanthanides. The results of experimental and theoretical calculations show that GDY has a significant effect on ion separation. It was noticed out that GDY has good mechanical properties[36] and there have been some studies on the application of copper foams coated GDY membranes for ion adsorption. In Liu's

5

RESEARCH ARTICLE

research[37], five pieces of GDY-based copper foam were stacked together and used as a filter for lead ions removal. When the solution was filtered five times, the lead ion concentration was reduced to as low as 0.02 mg/L reaching a removal efficiency of 99.6%. Moreover, the technology of membrane separation using copper foam as a separation membrane has been widely used[38]. Thus, it is very promising to use GDY membranes in the spent nuclear fuel reprocessing to achieve the separation between actinides and lanthanides with higher selectivity than ever before (Scheme 1).

Separation between Th^{4+} and UO$_2^{2+}$. Because it is hard to get a stable structure of UO$_2^{2+}$ adsorbed on GDY, both experimental and theoretical calculations proved that GDY has great potential for the selective separation between Th^{4+} and UO$_2^{2+}$. For Th^{4+} and UO$_2^{2+}$ coexisting in the nuclear fuel cycle, GDY membranes may be used to achieve completely separation between Th^{4+} and UO$_2^{2+}$.

Separation between Cs$^+$ and Sr^{2+}. Adsorption experiments have shown that GDY only adsorbed Cs$^+$ in the mixed solution of Cs$^+$ and Sr^{2+}, which is supported by the theoretical calculation that GDY cannot adsorb Sr^{2+} in the aqueous phase. It is believed that GDY has great potential to achieve complete separation between Cs$^+$ and Sr^{2+} in the aqueous phase. Thus, the strategy using GDY membrane to further separate Cs$^+$ and Sr^{2+}, which are extracted from high-level waste liquid, can be developed as an important supplement of the Advanced Nuclear Fuel Reprocessing.
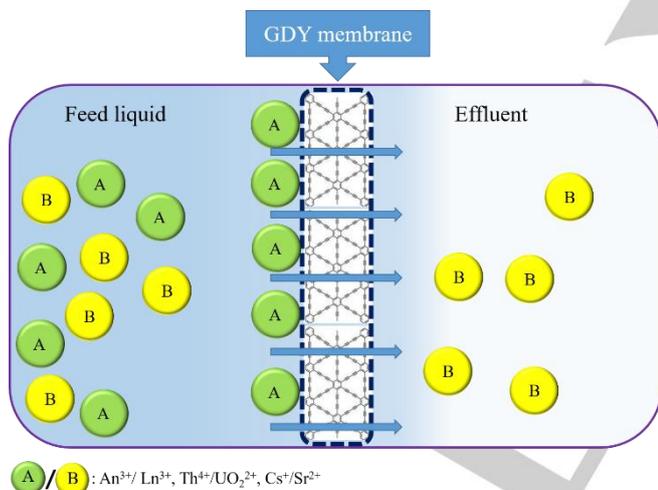
Scheme 1 Schematic diagram of GDY separation membrane.

Conclusion

In summary, GDY has been proven to have separation abilities between actinides and lanthanides, Th^{4+} and UO$_2^{2+}$, Cs$^+$ and Sr^{2+} through experiments and theoretical calculations. This complete separation performance makes GDY promising for its application in the nuclear fuel cycle. The deformations in the structure of GDY adsorbing actinides are essential for deep understanding its physicochemical properties. Moreover, further investigation on the basis of this work would reveal that GDY is a suitable substrate for actinides single ion.

[1] X. Gao, H. Liu, D. Wang, J. Zhang, *Chem. Soc. Rev.* **2019**, *48*, 908-936.
[2] G. Li, Y. Li, H. Liu, Y. Guo, Y. Li, D. Zhu, *Chem. Commun.* **2010**, *46*, 3256-3258.
[3] J. Zhou, X. Gao, R. Liu, Z. Xie, J. Yang, S. Zhang, G. Zhang, H. Liu, Y. Li, J. Zhang, Z. Liu, *J. Am. Chem. Soc.* **2015**, *137*, 7596-7599.
[4] R. Matsuoka, R. Sakamoto, K. Hoshiko, S. Sasaki, H. Masunaga, K. Nagashio, H. Nishihara, *J. Am. Chem. Soc.* **2017**, *139*, 3145-3152.
[5] a) C. Huang, Y. Li, N. Wang, Y. Xue, Z. Zuo, H. Liu, Y. Li, *Chem. Rev.* **2018**, *118*, 7744−7803. b) Y. Li, L. Xu, H. Liu, Y. Li, *Chem. Soc. Rev.* **2014**, *43*, 2572—2586. c) Y. Du, W. Zhou, J. Gao, X. Pan, Y. Li, *Acc. Chem. Res.* **2020**, *53*, 459−469.
[6] a) C. Huang, S. Zhang, H. Liu, Y. Li, G. Cui, Y. Li, *Nano Energy* **2015**, *11*, 481-489. b) H. Shang, Z. Zuo, L. Li, F. Wang, H. Liu, Y. Li, Y. Li, *Angew. Chem. Int. Ed. Engl.* **2018**, *57*, 774-778.
[7] a) R. Liu, H. Li, Y. Li, Y. Yi, X. Shang, S. Zhang, X. Yu, S. Zhang, H. Cao, G. Zhang, *Nanoscale* **2014**, *6*, 11336-11343. b) H. Yu, Y. Xue, L. Hui, C. Zhang, Y. Li, Z. Zuo, Y. Zhao, Z. Li, Y. Li, *Adv. Mater.* **2018**, *30*, 1707082. c) L. Hui, Y. Xue, B. Huang, H. Yu, C. Zhang, D. Zhang, D. Jia, Y. Zhao, Y. Li, H. Liu, Y. Li, *Nat. Coummun* **2018**, *9*, 5309.
[8] a) H. Li, R. Zhang, Y. Li, H. Liu, J. Shi, H. Zhang, H. Wu, Y. Luo, D. Li, Y. Li, Q. Meng, *Adv. Energy Mater.* **2018**, *8*, 1802012. b) X. Gao, H. Ren, J. Zhou, R. Du, C. Yin, R. Liu, H. Peng, L. Tong, Z. Liu, J. Zhang, *Chem. Mater.* **2017**, *29*, 5777-5781.
[9] a) C. Wang, P. Yu, S. Guo, L. Mao, H. Liu, Y. Li, *Chem. Commun.* **2016**, *52*, 5629-5632. b) N. Parvin, Q. Jin, Y. Wei, R. Yu, B. Zheng, L. Huang, Y. Zhang, L. Wang, H. Zhang, M. Gao, H. Zhao, W. Hu, Y. L. Li, D. Wang, *Adv. Mater.* **2017**, *29*, 1606755.
[10] J. Li, Y. Chen, J. Gao, Z. Zuo, Y. Li, H. Liu, Y. Li, *ACS Appl. Mater. Interfaces* **2018**, *11*, 2591-2598.
[11] C. Lu, Y. Yang, J. Wang, R. Fu, X. Zhao, L. Zhao, Y. Ming, Y. Hu, H. Lin, X. Tao, Y. Li, W. Chen, *Nat. Commun.* **2018**, *9*, 752.
[12] X. Li, D. Xing, *J. Phys. Chem.* **2019**, *123*, 8843-8850.
[13] D. Ma, T. Li, Q. Wang, G. Yang, C. He, B. Ma, Z. Lu, *Carbon* **2015**, *95*, 756-765.
[14] a) X. Yin, H. Wang, S. Tang, X. Lu, M. Shu, R. Si, T. Lu, *Angew. Chem. Int. Ed. Engl.* **2018**, *57*, 9382-9586. b) Y. Gao, Z. Cai, X. Wu, Z. Lv, P. Wu, C. Cai, *ACS Catal.* **2018**, *8*, 10364-10374. c) X. Li, S. Li, *J. Mater. Chem. C* **2019**, *7*, 1630-1640.
[15] a) K. Jeong, S. Park, S. Y. Lee, *J. Mater. Chem. A* **2019**, *7*, 1917-1935. b) J. Wang, W. Zhong, X. Liu, T. Yang, F. Li, Q. Li, W. Cheng, C. Gao, Z. Jiang, J Jiang, H. Cui, *Anal. Chem.* **2017**, *89*, 13518-13523.
[16] G. Simon, A. A. McAdams, A. K. Kostopoulos, P. S. James, F. T. Walsh, *Coordin. Chem. Rev.* **2017**, *346*, 216-239.
[17] a) B. Arunasis, K. M. Prasanta, *Radiochim. Acta* **2019**, *107*, 931-949. b) R. Malmbeck, C. Nourry, M. Ougier, P. Soucek, J. P. Glatz, T.Kato, T.Koyama, *Energy Procedia,* **2011**, *7*, 93-102.
[18] a) S. Manohar, J. N. Sharma, B. V. Shah, P. K. Wattal, *Nucl. Sci. Eng.* **2007**, *156*, 96-102. b) E. A. Mowafy, *Radiochim. Acta* **2007**, *95*, 539-545. c) C. Marie, M. Miguirditchian, D. Guillaumont, A. Tosseng, C. Berthon, P. Guilbaud, M. Duvail, J. Bisson, D. Guillaneux, M. Pipelier, D. Dubreuil, *Inorg. Chem.* **2011**, *50*, 6557-6566. d) M. Galletta, S. Scaravaggi, E. Macerata, A. Famulari, A. Mele, W. Panzeri, F. Sansone, A. Casnati, M. Mariani, *Dalton Trans.* **2013**, *42*, 16930-16938.
[19] a) M. G. B. Drew, M. J. Hudson, P. B. Iveson, C. Madic, M. L. Russell, *J. Chem. Soc. Dalton Trans.* **2000**, *16*, 2711-2720. b) S. Trumm, A. Geist, P. J. Panak, T. Fanghanel, *Solvent Extr. Ion Exc.* **2011**, *29*, 213-229. c) F. W. Lewis, L. M. Harwood, M. J. Hudson, M. G. B. Drew, J. F. Desreux, G. Vidick, N. Bouslimani, G. Modolo, A. Wilden, M. Sypula, T. H. Vu, J. P. Simonin, *J. Am. Chem. Soc.* **2011**, *133*, 13093-13102.
[20] a) D. D. Ensor, G. D. Jarvinen, B. F. Smith, *Solvent Extr. Ion Exc.* **1988**, *6*, 439-445. b) X. Wang, Y. Zhu, R. Jiao, *Solvent Extr. Ion Exc.* **2001**,

19, 1007-1015. c) G. Modolo, P. Kluxen, A. Geist, *Radiochim. Acta* **2010**, *98*, 193-202.

[21] a) E. P. Horwitz, D. R. McAlister, A. H. Bond, R. E. Barrans, *Solvent Extr. Ion Exch.* **2005**, *23*, 319-344. b) Ch. Siva Kesava Raju, M. S. Subramanian, *Sep. Purif. Technol.* **2007**, *55*, 16-22. c) Ch. Siva Kesava Raju, M. S. Subramanian, *J. Hazard. Mater.* **2007**, *145*, 315-322.

[22] a) P. W. Naik, P. S. Dhami, S. K. Misra, U. Jambunathan, J. N. Mathur, *J. Radioanal. Nucl. Chem.* **2003**, *257*, 327-332. b) A. Zhang, E. Kuraoka, M. Kumagai, *Sep. Purif. Technol.* **2007**, *54*, 363-372.

[23] a) S. A. Ansari, P. N. Pathak, M. Husain, A. K. Prasad, V. S. Parmar, V. K. Manchanda, *Talanta* **2006**, *68*, 1273-1280. b) A. Bhattacharyya, P. K. Mohapatra, V. K. Manchanda, *J. Chromatogr. A* **2006**, *1123*, 26-30.

[24] Z. Zhu, Y. Pranolo, C. Y. Cheng, *Miner. Eng.* **2015**, *77*, 185–196.

[25] a) C. L. Riddle, J. D. Baker, J. D. Law, C.A. McGrath, D. H. Meikrantz, B. J. Mincher, D. R. Peterman, T. A. Todd, *Solvent Extr. Ion Exch.* **2005**, *23*, 449–461. b) L. H. Delmau, P. V. Bonnesen, N. L. Engle, T. J. Haverlock, F. V. Sloop, B. A. Moyer, *Solvent Extr. Ion Exch.* **2006**, *24*, 197–217. c) O. Halevi, T. Y. Chen, P. S. Lee, S. Magdassi, J. A. Hriljac, *RSC Adv.* **2020**, *10*, 5766-5776.

[26] C. Xu, J. Wang, J. Chen, *Solvent Extra. Ion Exc.* **2012**, *30*, 623–650.

[27])a) G. X. Tian, J. C. Wang, Y. F. Shen, L. F. Rao, *Solvent Extr. Ion Exch.* **2005**, *23*, 519–528. b) B. Gruner, J. Plesek, J. Baca, J. F. Dozol, V. Lamare, I. Cisarova; M. Belohradsky, J. Caslavsky, *New J. Chem.* **2002**, *26*, 867–875.

[28] a) A. Casnati, S. Barboso, H. Rouquette, M. J. Schwing-Weill, F. Arnaud-Neu, J. F. Dozol, R. Ungaro, *J. Am. Chem. Soc.* **2001**, *123*, 12182–12190. b) B. W. Harmon, D. D. Ensor, L. H. Delmau, B. A. Moyer, *Solvent Extr. Ion Exch.* **2007**, *25*, 373–388.

[29] a) A. Das, C. Dash, M. A. Celik, Yousufuddin, M., Frenking, G. & Dias, H. V. R. *Organometallics* **2013**, *32*, 3135-3144. b) J. D. Ferrara, Y. C. Tessier, W. J. Youngs, *Organometallics* **1987**, *6*, 676-678.

[30] N. Heinz, J. Zhang, M. Dolg, *J. Chem. Theory. Comput.* **2014**, *10*, 5593-5598.

[31] Y. J. Marcus, *Chem. Soc. Faraday Trans.* **1991**, *87*, 2995-2999.

[32] a) L. Hui, Y. Xue, H. Yu, Y. Liu, Y. Fang, C. Xing, B. Huang, Y. Li, *J. Am. Chem. Soc.* **2019**, *141*, 10677-10683. b) Y. Xue, B. Huang, Y. Yi, Y. Guo, Z. Zuo, Y. Li, Z. Jia, H. Liu, Y. Li, *Nat. Commun.* **2018**, *9*, 1460. c) J. He, S. Y. Ma, P. Zhou, C. X. Zhang, C. He, L. Z. Sun, *J. Phys. Chem. C* **2012**, *116*, 26313−26321.

[33] K. Yang, J. Lee, H. Choo, F. Yang, *J. Phys. Chem. C* **2018**, *122*, 24467-24474.

[34] J. W. Charles, J. M. Tobin, *Dalton Trans.* **2010**, *39*, 6576–6588.

[35] a) S. Jiang, B. Wang, H. Sun, Z. Wang, S. Gao, *J. Am. Chem. Soc.* **2011**, *133*, 4730-4733. b) S. Jiang, S. Liu, L. Zhou, B. Wang, Z. Wang, S. Gao, *Inorg. Chem.* **2012**, *51*, 3079-3087.

[36] a) F. Bruno, S. Nuno, N. C. L. José, *Comp. Mater. Sci.* **2020**, *171*, 109233.b) D. Solis, D. Borges, C. Woellner, D. Galvão, *ACS Appl. Mater. Interfaces* **2019**, *11*, 2670−2676.

[37] R. Liu, J. Zhou, X. Gao, J. Li, Z. Xie, Z. Li, S. Zhang, L. Tong, J. Zhang, Z. Liu, *Adv. Electron. Mater.* **2017**, *3*, 1700122.

[38] a) Y. Hou, M. Liu, L. Zhang, M. Li, D. Wang, J. Liu, S. Fu, *Sep. Purif. Technol.* **2020**, *240*, 116598. b) Y. Zhang, J. Yang, L. Li, C. Cui, Y. Li, S. Liu, X. Zhou, L. Qu, *Polymers* **2019**, *11*, 97. c) J. Du, C. Zhang, H. Pu, Y. Li, S, Jin, L. Tan, C. Zhou, L. Dong. *Colloid Surf. A-Physicochem. Eng. Asp.* **2019**, *573*, 222–229.

WILEY-VCH

RESEARCH ARTICLE

Entry for the Table of Contents

A / B An^{3+}/Ln^{3+}, Cs^+/Sr^{2+}, Th^{4+}/UO_2^{2+}
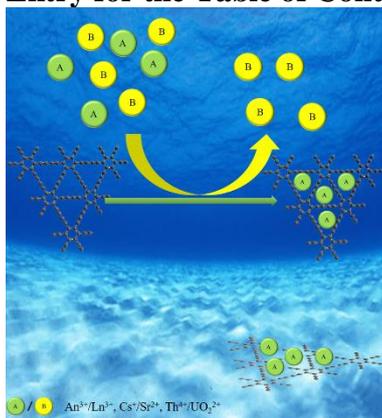
Graphdiyne provides a new strategy on separation between actinides and lanthanides, Th^{4+} and UO_2^{2+}, Cs^+ and Sr^{2+}, in which actinides or Cs^+ adsorbed on graphdiyne are in the single ion state.